

Journal of Materials Chemistry A

Accepted Manuscript



This is an *Accepted Manuscript*, which has been through the Royal Society of Chemistry peer review process and has been accepted for publication.

Accepted Manuscripts are published online shortly after acceptance, before technical editing, formatting and proof reading. Using this free service, authors can make their results available to the community, in citable form, before we publish the edited article. We will replace this *Accepted Manuscript* with the edited and formatted *Advance Article* as soon as it is available.

You can find more information about *Accepted Manuscripts* in the [Information for Authors](#).

Please note that technical editing may introduce minor changes to the text and/or graphics, which may alter content. The journal's standard [Terms & Conditions](#) and the [Ethical guidelines](#) still apply. In no event shall the Royal Society of Chemistry be held responsible for any errors or omissions in this *Accepted Manuscript* or any consequences arising from the use of any information it contains.



Journal Name

ARTICLE

A Wearable and Highly Sensitive CO Sensor with Macroscopic Polyaniline Nanofiber Membrane

Anoscale Received 00th January 20xx,

Accepted 00th January 20xx

DOI: 10.1039/x0xx00000x

www.rsc.org/

Jingjing Zhao,^a Guan Wu,^a Ying Hu,^a Yang Liu,^a Xiao-ming Tao^b and Wei Chen^{*a}

Wearable CO sensor based on macroscopic membrane which consists of polyaniline (PANI) coating electrospun nanofibers is reported. The membrane material owns a centimeter range macro film shape with highly porous networks and ultra-fine nanofibers structure modified with PANI nanocone by in-situ polymerization route, making it suitable candidate for sensing materials. Sensors based on the macro PANI nanofiber membrane is constructed, displaying rapidly responses (20s) for CO with high detection limits (2.5 ppb) at room temperature. Furthermore, by replacing nanofibers template with natural cotton fibers, sensing material towards wearable sensor is manufactured and excellent sensing responses are also detected. This work provides a simple process to make macroscale sensing material with homogeneous, subtle nanoscale architecture and offer significant opportunities for wearable sensors.

Introduction

These is a growing interest on wearable electronics due to the novel features such as flexibility, light-weight, stretchability, and wide applications in health personal healthcare, environmental monitoring and energy harvesting.¹⁻⁴ As an important function of the wearable electronics, real-time detection of low-concentration harmful gases effectively has received enormous interests as a result of the increased threat of the air pollutant.⁵ It is highly desirable to develop some flexible, stretchable and room-temperature sensors that are readily incorporated with the wearable systems, such as the fabrics or clothing worn by human in daily life.^{6,7}

Flexible conducting polymer based chemiresistor is a significant class of sensors that fulfill these requirements and is displaying promising performance in a variety of wearable sensing applications.⁸ Polyaniline (PANI), one of the most studied electrically conductive polymers, has been widely recognized as a highly sensitive material because its electric conductivity is easily modified with the chemical environment change after doping or adsorption.⁹ Different PANI-based sensors, including PANI films,^{10, 11} PANI composites¹²⁻¹⁴ and PANI nanowires,¹⁵ have been extensively investigated in recent years. Among these, the nanostructured PANI integrated electronic devices are usually fabricated on the rigid substrates through complicated semiconductor micromachining process, including lithography, annealing, deposition and packaging,¹⁶⁻¹⁹ which obviously limits the real development and application of sensors towards wearable electronic system. On the other hand,

those PANI sensors which have been fabricated in large scale, such as PANI films or PANI composites, presently still suffered from their relatively low sensitivity due to the poor contact area and low reactivity. Therefore, it is particularly urgent to develop some flexible, subtle nanoscale sensing architectures in a simple and compatible manner for wearable systems.

Fiber nanostructure fabricated by electrospinning has been studied as a promising sensing architecture due to its high specific surface area, and ease fabrication to form macroscale flexible and breathable fabrics.²⁰⁻²² These features may open up the potential application of the fiber structures in wearable gas sensors. Here considering the fact that the PANI is a little difficult to be processed by electrospinning due to its low viscoelasticity,⁹ in this experiment PANI was in-situ polymerized on an electrospun polyacrylonitrile (PAN) nanofiber membrane. The membrane which was made by PAN nanofibers ranging from tens of nanometers to several micrometers in diameter, served as the porous scaffold with high specific surface area for gas penetration. In order to achieve the high level active sites for gas sensing, fine PANI nanostructure addressed on the surface of PAN nanofiber was then successfully fabricated and adjusted by the proportion of aniline and dopant. Typically, a uniform PANI nanocone layer is produced on each PAN nanofiber. As expected, the resultant macroscale composite membrane is flexible and can be easily transferred onto any substrates. Surprisingly, highly sensing performance towards CO is demonstrated, displaying rapid response (20 s) with high detection limits (2.5 ppb) at room temperature. Except for the PAN nanofiber membrane, the PANI addressed cotton fabric is also demonstrated as a reactive sensing framework. It is justified to believe that this simple and versatile approach by functional nanomaterial coated fibers and fiber network will provide an applicable research and development platform for wearable electronics.

^a *i-Lab, Suzhou Institute of Nano-tech and Nano-bionics, Chinese Academy of Sciences, Suzhou 215123, P. R. China. E-mail: wchen2006@sinano.ac.cn*

^b *Nanotechnology Center, Institute of Textiles and Clothing, The Hong Kong Polytechnic University, Kowloon, Hong Kong SAR, P. R. China.*

Electronic Supplementary Information (ESI) available

Results and discussion

The fabrication of PANI coated PAN nanofiber membrane is depicted in Fig. 1. Firstly, a PAN nanofiber based template is prepared by electrospinning as it is one of the simplest, versatile and low-cost methods for mass-production. As seen in the SEM image (Fig. 1a), the PAN template shows a porous network consisting of numerous individual nanofibers with smooth surface structure, and its macroscopic film on aluminum foil is given in the inset of Fig. 1a. Secondly, by a facile chemical polymerization method, in which aniline acts as reactant, 5-sulfosalicylic acid dehydrate (SSA) acts as dopant and ammonium persulfate (APS) acts as oxidant. This in-situ reaction process could not only greatly enhance the adhesion between PANI coated layer and PAN nanofiber template but also improve the regularity of PANI morphology, as shown in Figure 1b. Obviously, PANI are in-situ coated on the PAN nanofibers, which displays a good homogeneity along the whole nanofibers, Enlarged microstructure of the PANI coated fiber is shown in the inset of Fig. 1b. Distinctive PANI nanocone layer is produced.

As known, during PANI polymerization process, the chemical doping plays an important role in PANI electrical property and then sensing performance. In our experiment, it is found the doping also generate remarkable effect on the morphology of the formed PANI nanostructure. Microstructure evolution as a function of the doping level is exhibited by SEM and TEM images as shown in Fig. 2. At the low molar ratio of SSA and PANI (0.2), the fiber surface turns to be rough, and fiber diameter is found to be around 120 nm, as shown in Fig. 2a. The inset TEM picture in Fig. 2a displays that only a few indistinct nanocones with a small size form, indicating a very thin layer of coating. However, with the molar ratio increased to 0.8 and 1, spinous nanocones feature of PANI become distinct, and corresponding fiber diameters increase to be between 250 nm to 300 nm, as shown in Fig. 2b and 2c. The unique structure can be clearly evidenced by the inset TEM images, in which the rod-like PANI nanocones are densely

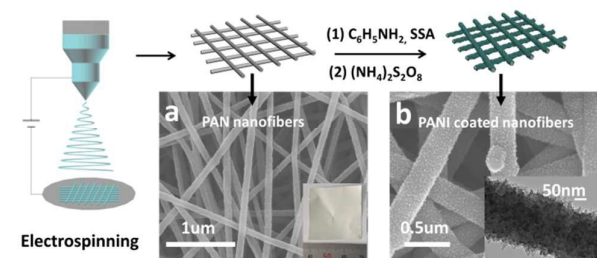


Fig. 1. PANI coated nanofibers fabrication process from electrospun PAN nanofibers.

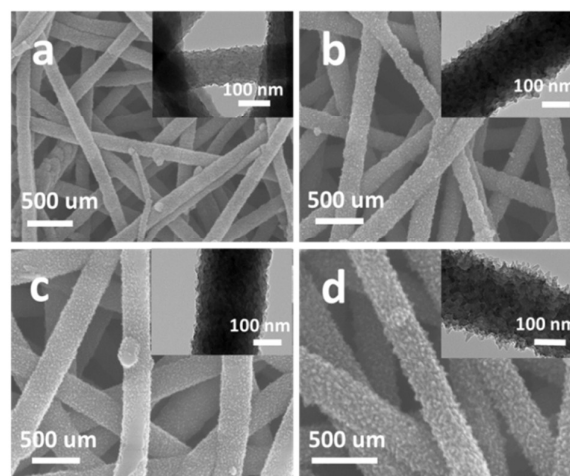


Fig. 2. SEM and TEM images of PANI coated nanofibers with different doping levels. (a) $[SSA] / [ANI] = 0.2$; (b) $[SSA] / [ANI] = 0.8$; (c) $[SSA] / [ANI] = 1$; (d) $[SSA] / [ANI] = 2$;

grafted throughout the whole nanofibers. As the molar ratio further increased to 2, Fig. 2d shows that the PAN fiber is then fully covered with vertically grown PANI nanocones in uniform size and shape, with a diameter of 350 nm approximately. Apparently, the PANI nanostructure and resultant functional coating on PAN nanofibers can be easily tuned and controlled with different SSA doping levels during polymerization. The spinous nanostructure will increase surface areas, as shown in Table S1.

The PANI coated nanofiber is then confirmed by Raman spectra and FTIR spectra, as shown in Fig. S1. In Fig. S1a, typical absorption peaks at 1167 cm^{-1} , 1335 cm^{-1} , 1488 cm^{-1} , 1601 cm^{-1} correspond to C-H bending of benzene ring, C-N stretching of benzene ring, C=C stretching of benzene ring, and as well as C=C stretching of quinoid ring respectively. Fig. S1b shows the Fourier transform infrared (FTIR) spectroscopy of these membranes. It is found that PANI nanofiber have characteristic peaks at around 1588 cm^{-1} , 1502 cm^{-1} , 1308 cm^{-1} , 1150 cm^{-1} , 829 cm^{-1} . These bands are associated with C=C stretching deformation of quinoid ring, C=C stretching deformation of benzene ring, C-N stretching of benzene ring and out-of-plane deformation of benzene ring. All the information demonstrates PANI layer with different doping levels had successfully coated on the surface of PAN nanofibers.

In order to study the sensing properties of macroscale nanofiber membrane, every sample was cut in the size of $12\text{ mm} \times 3\text{ mm}$ and transferred to a PCB board with built-in conducting wires and electrodes. An exemplary picture of the constructed macroscale membrane sensor is presented in the inset of Fig. 3a. Details about the sensor fabrication and sensing setup are clearly described in the experimental section. Resultantly, when the macroscale membrane is exposed to CO gas, high sensing performance with rapid response and extremely low detection limit at room temperature, is demonstrated. Representative

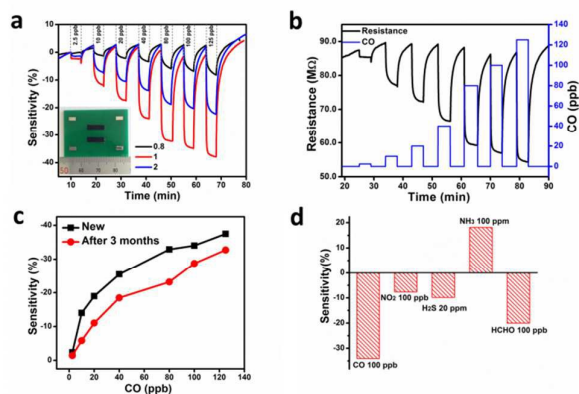


Fig. 3. (a) Comparison in sensitivity of PANI sensors with different doping level to CO (inset: PANI sensor based on rigid PCB substrate). (b) Dynamic response of PANI sensor with mole ratio of 1 to different concentrations of CO at room temperature on PCB substrate. (c) Comparison in sensitivities of sensors before and after storage in air for 3 months. (d) Selectivity of PANI sensor to different gases.

sensitivity results of the membrane sensors with different SSA doping levels are presented in Fig. 3a. During exposure to CO concentrations ranging from 2.5 ppb to 125 ppb, we find when the sample with SSA doping level is low, such as at ratio of 0.2, there is no gas sensing signal due to the likely high resistance of PANI. While other sensors with ratios of 0.8, 1 and 2, totally present to be sensitive to CO and display well-resolved reversible response signals in the above CO concentration range. Interestingly, although the sensor has the middle SSA doping level, such as at ratio of 1, it displays the best sensitivity, a 2-4 fold increase in sensitivity compared to the sensors with ratio of 0.8, and 2 respectively. For the sensor with higher ratio of 2, it only shows the decreased sensitivity. Such difference can be rationalized by the different quantity of Q-N (nitrogen atoms in quinoid diamine) and B-N (nitrogen atoms in benzenoid diamine) of the PANI polymer with different doping levels. Generally, in the protonating doping process, hydrogen ions will react with nitrogen atoms and the resulting polymer could conduct electrons in sensing process (Fig. S2).²³ It is important to note that hydrogen ions are more eager to interact with Q-N than B-N in this process. Therefore, only Q-N accepts hydrogen ions when there is a small amount of acid. However, with a high acid content, B-N would combine with hydrogen ions and decrease in quantity after Q-N reacts to completion.²⁴ However, in the sensing process, B-N is supposed to be the interaction active site between PANI and CO, and then influence the gas sensitivity.²³ On the other words, an increased doping level would lower the gas sensitivity. In conclusion, a low doping level leads the PANI material a poor electrical conductivity, making it unsuitable for resistive sensor. Therefore, the sensitivity of sensor with ratio of 0.8 is lower than sensor with ratio of 1. Nevertheless, high doping level will decrease the active sites in CO detection, resulting in a reduction in sensitivity of sensor with ratio 2.

There should be a modest doping level for PANI that not only exists more active sites but also maintains good material conductance. Obviously, PANI sensor with SSA doping molar ratio of 1 in our experiment exhibits the best performance.

Fig. 3b is the dynamic response of PANI sensor with molar ratio of 1 to different concentrations of CO. It is noteworthy that the acid doped PANI exhibits p-type semiconductor characteristics.²⁵ So exposing to CO will lead to increase in charge-carrier concentrations and decrease in resistance of the sensor due to lone pair electron shift.²⁶ As shown in the diagram, when CO passes through, the resistance of sensor almost vertically decreases initially and then gradually achieves its steady state, in accordance with the electrical characteristic of PANI. After dry air purging, the resistance quickly increases and gradually recovers back to its initial level. A normalized sensitivity of 37% for 125 ppb CO, and 2% for ultra-low CO concentration (2.5 ppb) are obtained. Meanwhile fast response is discovered that the response time is less than 20 seconds while recovery time is about 50 seconds. These are quite excellent results for non-noble metal based sensors operating at room temperature. The high sensing performance can be attributed to the unique surface nanostructure of the nanofiber membrane and physical interaction mechanism between PANI molecule and CO molecule. Porous network of electrospun nanofibers facilitates effective penetration of the surrounding CO gas. Moreover, densely assembled PANI nanocones on the nanofibers further enhance the contact area at the interface between sensing material and pollution gas, which raises sensitivities. On the other side, CO has stable resonance [$+C\equiv O-$], with a positive charge at the carbon atom, which tends to attract a lone pair electron at the nitrogen in the sensing process.²⁷ The sensing mechanism could be concluded by the electron transfer between PANI and CO molecule, which consequently changed the chemical resistance of PANI. Hence, the physical electron shift between CO and PANI results in pollution air going through a fast adsorption and desorption process,²⁸ which is consistent with the fast and reversible responses discussed above. Apart from the high specific surface area of PANI nanofibers membrane, we assume that the high sensitivity was caused by the influence of dopant (5-sulfosalicylic acid dehydrate) making specifically bonding with the CO.

Sensor stability is another key criterion for sensing properties. Fig. 3c illustrates the sensing performance after being placed in air for about 3 months. The sensor still work well after long time storage with good reversibility and fast response, and only shows a little decrease in sensitivities, indicating that the macro PANI coated nanofiber membrane based sensors have good stability in long time use. In addition, the selectivity of our sensor also be studied and different gases are used to measure the performance, as demonstrated in Fig. 3d. NO_2 is a strong electron-withdrawing molecule,²⁹ and it tends to interact with the lone-pair electrons of nitrogen atom in the benzenoid diamine so it exhibits a negative response signal. On the contrary, the response curves shows positive signal in NH_3 sensing as NH_3 is a strong electron-donating molecule and it

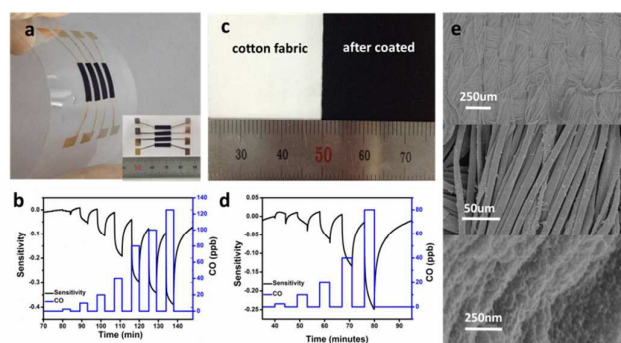


Fig. 4. (a) PANI sensor based on flexible PET substrate. (b) Dynamic response of PANI sensor to different concentrations of CO at room temperature on the PET substrate. (c) Digital image of cotton fabric before and after PANI coating. (d) Dynamic response of PANI coated cotton fabric sensor to different concentrations of CO at room temperature. (e) SEM images of PANI coated cotton fabric.

would transfer electrons to nitrogen atom. HCHO are similar molecules to NO_2 , thus the PANI sensor exhibits a similar sensing signals. There is a small response to H_2S because it is a weak acid.

These wearable electronics represent an important application area that can be realized using the PANI coated nanofiber membrane. For these investigations, the macro membrane (12mm×3mm) is transferred onto a flexible polyethylene terephthalate (PET) film with Au arrays which serve as electrodes. Fig. 4a demonstrates that the sensing materials transferred to the PET film can be bent to a small angle without cracking, indicating the excellent mechanical flexibility of our material. The real-time sensing property is also investigated (Fig. 4b) and similar curve is obtained comparing to data in Fig. 3b, showing its potential in wearable application. Environmental monitoring devices mounted on human clothing are of great interest, and efforts to integrate sensing devices with human garment also have conducted in this paper. As an alternative strategy, a natural cotton fabric made in industrial textile technology is used as template for PANI coating, and the obtained material is revealed in Fig. 4c. Comparing the white template in left, the fabric turns to be dark blue because of PANI coating, as shown in the optical picture. SEM images (Fig. 4e) indicate that uniform PANI coated layer has formed onto the flexible, free-standing cotton fabric, by the same polymerization process. This process enables strong binding between PANI coating layer and cotton fiber and outstanding mechanical flexibility of the composite materials, which will enhance stability in using. Also, the cotton fabric retains its construction after reaction and allows them to integrate directly onto garment, in a conformal manner. In the real-time CO sensing test (Fig. 4d), the output signal shows excellent response to CO as well. This approach is especially promising for the real-time detection of poisonous gas within areas that are inevitably confronted with people.

Conclusions

In conclusion, the work presented here demonstrates the in-situ polymerization of PANI on electrospun nanofibers to form a macroscopic membrane with inside nanostructure and its application for the wearable gas sensing. This synthesis approach exhibits a subtle architecture composed of high-quality PANI nanocones anchored on the PAN backbone. The sensor based on flexible macroscopic membrane with simple device configuration shows effective signal to toxic CO at room temperature with the concentrations as low as 2.5 ppb. Our approach could also be applied to natural fibers such as cotton fibers, which offered unique potential for wearable electronics devices. Furthermore, this simple and versatile method of chemical coating on nanofiber template for introducing functionalities for sensing application will provide a foundation for intelligent and wearable electronic sensors.

Experimental

Polyacrylonitrile (PAN, $M_w=50\ 000$), 5-sulfosalicylic acid dehydrate (SSA), Ammonium persulfate (APS), N, N-Dimethyl formamide (DMF), aniline monomer were purchased from Sinopharm Chemical Reagent Co., Ltd. Aniline monomer was distilled under reduced pressure and stored below 0°C before use.

Electrospun PAN nanofiber membrane

PAN was added into DMF with the concentration of 0.08 g/mL followed by magnetic stirring for 6 h to obtain a homogenous solution. The solutions were loaded into a 2 ml plastic syringe and pumped through a syringe pump in the electrospinning apparatus at a rate of 0.1 mL/min. The applied voltage was 14 kV, and the distance between the spinneret and collection plate was 8 cm. After 90 minutes a PAN nanofiber membrane was formed, then the membrane was dried in air for one day in order to remove any residual DMF.

Polymerization of PANI

50 μL aniline was added slowly to 10 mL deionized water with different quantities SSA, followed by magnetic stirring for 1 h. Subsequently the PAN nanofiber membrane was immersed the solutions for 4 h. After that, 10 mL 0.05mol/L APS aqueous solutions was added and kept in $0-5^\circ\text{C}$ for 14 h. Finally, the products were cleaned with deionized water and ethanol. A composite macro nanofiber membrane with uniform PANI coating was formed. The preparation of PANI coated cotton fabric was carried out by the same method as described above except that cotton fabric instead of PAN nanofibers membrane.

Characterization

The surface images of nanofiber membrane were obtained by transmission electron microscopy (FEI, 200KV) and FESEM (Hitachi S-4800). Fourier-transform infrared (FTIR) spectroscopy measurement was performed using a Thermo FTIR spectrometer. Raman Spectra were recorded by a Jobin-Yvon LabRam HR 800 confocal micro-Raman system equipped with an electrically-cooled detector. The excitation wavelengths were 532 nm with a Nd:YAG laser.

Sensor device fabrication

The sensor prototype was a simple homemade PCB circuit board comprising built-in conducting wires which contacted with four electrodes. The space between these two electrodes is 10 mm. The PANI nanofiber membrane was cut into small samples size of 3 mm × 12 mm using as sensing sample which was attached to the electrodes on the substrates. To allow the sample to contact electrodes closely, the silver paste was used to fix the ends of samples; The PET (polyethylene terephthalate) film with gold (Ag) electrodes was used as a flexible substrate in this study.

Sensing tests

The detailed gas sensing experimental setup was similar to previous work. Briefly, the measurement was conducted using a WS-30A system (Weisheng Instruments Co., Zhengzhou, China). Dry air or air/CO gas was fixed at a flow rate of 200 sccm (cubic centimeter per minute at STP) using mass flow controllers (Beijing Sevenstar Electronics Co., Ltd). A 2 V DC potential was applied to the circuit and a custom Labview computer program was employed to continuously monitor the sensor's resistance change using the field-point analog input and output modules. The sensitivity is defined as $S = (R_g - R_a)/R_a$, where R_a is the electrical resistance in the air and R_g is the electrical resistance in the pollution gas. All the tests were conducted at room temperature. The response time is defined as the time required for the resistance change to reach within 1/e of the total change between steady state values obtained during exposure and purging.

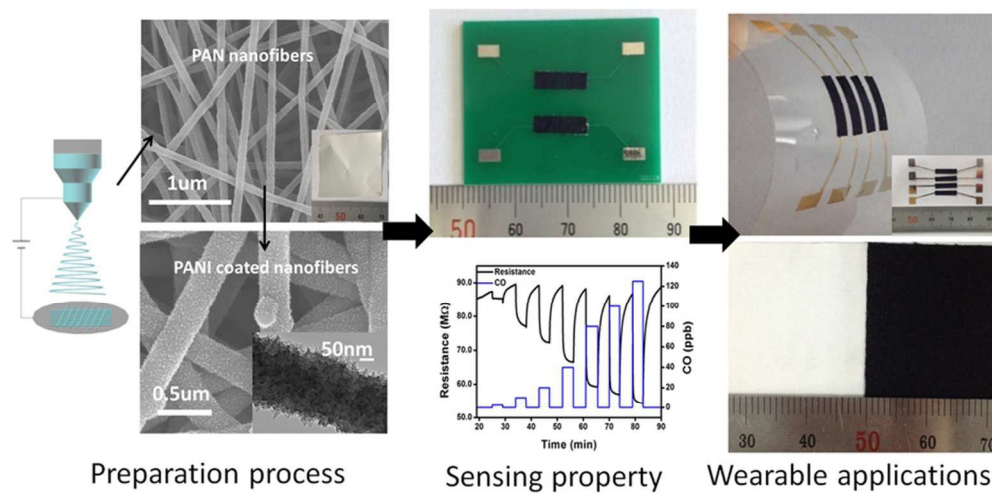
Acknowledgements

This work was supported by the Natural Science Foundation for Distinguished Young Scientists of Jiangsu Province (BK2012008), the Hong Kong, Macao and Taiwan Science and Technology Cooperation Program of China (2012DFH50120), the National Natural Science Foundation of China (21373263) and the External Cooperation Program of BIC, Chinese Academy of Sciences (121E32KYSB20130009).

Notes and references

- 1 W. Zeng, L. Shu, Q. Li, S. Chen, F. Wang and X. M. Tao, *Adv. Mater.*, 2014, **26**, 5310-5336.

- 2 B. Sun, Y.-Z. Long, Z.-J. Chen, S.-L. Liu, H.-D. Zhang, J.-C. Zhang and W.-P. Han, *J. Mater. Chem. C*, 2014, **2**, 1209-1219.
- 3 C. Pang, C. Lee and K.-Y. Suh, *J. Appl. Polym. Sci.*, 2013, **130**, 1429-1441.
- 4 M. L. Hammock, A. Chortos, B. C. Tee, J. B. Tok and Z. Bao, *Adv. Mater.*, 2013, **25**, 5997-6038.
- 5 X. Liu, S. Cheng, H. Liu, S. Hu, D. Zhang and H. Ning, *Sensors*, 2012, **12**, 9635-9665.
- 6 K. Saetia, J. M. Schnorr, M. M. Mannarino, S. Y. Kim, G. C. Rutledge, T. M. Swager and P. T. Hammond, *Adv. Funct. Mater.*, 2014, **24**, 492-502.
- 7 S. Park, M. Vosguerichian and Z. Bao, *Nanoscale*, 2013, **5**, 1727-1752.
- 8 C. M. Hangarter, N. Chartuprayoon, S. C. Hernández, Y. Choa and N. V. Myung, *Nano Today*, 2013, **8**, 39-55.
- 9 Y. Zhang, J. J. Kim, D. Chen, H. L. Tuller and G. C. Rutledge, *Adv. Funct. Mater.*, 2014, **24**, 4005-4014.
- 10 S. Srinives, T. Sarkar and A. Mulchandani, *Electroanalysis*, 2013, **25**, 1439-1445.
- 11 S. H. Hosseini, R. Ansari and P. Noor, *Phosphorus, Sulfur, and Silicon and the Related Elements*, 2013, **188**, 1394-1401.
- 12 M. Ding, Y. Tang, P. Gou, M. J. Reber and A. Star, *Adv. Mater.*, 2011, **23**, 536-540.
- 13 K. H. An, S. Y. Jeong, H. R. Hwang and Y. H. Lee, *Adv. Mater.*, 2004, **16**, 1005-1009.
- 14 C. Li, N. Chartuprayoon, W. Bosze, K. Low, K. H. Lee, J. Nam and N. V. Myung, *Electroanalysis*, 2014, **26**, 711-722.
- 15 E. Song and J.-W. Choi, *Nanomaterials*, 2013, **3**, 498-523.
- 16 X. Zhao, B. Cai, Q. Tang, Y. Tong and Y. Liu, *Sensors*, 2014, **14**, 13999-14020.
- 17 L. Li, P. Gao, M. Baumgarten, K. Müllen, N. Lu, H. Fuchs and L. Chi, *Adv. Mater.*, 2013, **25**, 3419-3425.
- 18 Y. Liu, Z. Jin, J. Wang, R. Cui, H. Sun, F. Peng, L. Wei, Z. Wang, X. Liang, L. Peng and Y. Li, *Adv. Funct. Mater.*, 2011, **21**, 986-992.
- 19 P. C. Chen, S. Sukcharoenchoke, K. Ryu, L. Gomez de Arco, A. Badmaev, C. Wang and C. Zhou, *Adv. Mater.*, 2010, **22**, 1900-1904.
- 20 A. Greiner and J. H. Wendorff, *Angew. Chem. Int. Ed.*, 2007, **46**, 5670-5703.
- 21 J. Wu, N. Wang, Y. Zhao and L. Jiang, *J. Mater. Chem. A.*, 2013, **1**, 7290.
- 22 D. Li and Y. Xia, *Adv. Mater.*, 2004, **16**, 1151-1170.
- 23 H. Bai, and G. Shi, *Sensors*, 2007, **7**, 267-307.
- 24 Y. Liao, C. Zhang, Y. Zhang, V. Strong, J. Tang, X. G. Li, K. Kalantar-Zadeh, E. M. Hoek, K. L. Wang and R. B. Kaner, *Nano Lett.*, 2011, **11**, 954-959.
- 25 G. Ćirić-Marjanović, *Synthetic Metals*, 2013, **177**, 1-47.
- 26 H. H. Choi, J. Lee, K.-Y. Dong, B.-K. Ju and W. Lee, *Macromolecular Research*, 2012, **20**, 143-146.
- 27 S. Watcharaphalakorn, L. Ruangchuay, D. Chotpattananont, A. Sirivat and J. Schwank, *Polymer International*, 2005, **54**, 1126-1133.
- 28 H. Ullah, A.-u.-H. A. Shah, S. Bilal and K. Ayub, *J. Phys. Chem. C*, 2013, **117**, 23701-23711.
- 29 D. H. Wang, Y. Hu, J. J. Zhao, L. L. Zeng, X. M. Tao and W. Chen, *J. Mater. Chem. A*, 2014, **2**, 17415-17420.



39x19mm (600 x 600 DPI)